

Intrinsic biophysical diversity decorrelates neuronal firing while increasing information content

Krishnan Padmanabhan^{1,2} & Nathaniel N Urban^{1–3}

Although examples of variation and diversity exist throughout the nervous system, their importance remains a source of debate. Even neurons of the same molecular type have notable intrinsic differences. Largely unknown, however, is the degree to which these differences impair or assist neural coding. We examined the outputs from a single type of neuron, the mitral cells of the mouse olfactory bulb, to identical stimuli and found that each cell's spiking response was dictated by its unique biophysical fingerprint. Using this intrinsic heterogeneity, diverse populations were able to code for twofold more information than their homogeneous counterparts. In addition, biophysical variability alone reduced pair-wise output spike correlations to low levels. Our results indicate that intrinsic neuronal diversity is important for neural coding and is not simply the result of biological imprecision.

From the earliest drawings of neurons¹ to the identification of families of voltage-gated ion channels², a central theme of neuroscience has been the marked intrinsic variety of cells. While catalogs of types of neurons continue to grow³, the importance of intrinsic diversity within neurons of a single type for neuronal coding has been largely ignored. Differences in channel expression and morphology^{4,5} can diversify spike outputs, even among cells of a single identified type⁶. Alternatively, spiking properties can be equivalent among neurons with channel densities of different proportions⁶. Intrinsic variability therefore seems to have multiple roles in mechanisms of spike generation. However, the extent to which these individual differences in cells are relevant to neural coding is less well understood.

Intrinsic diversity could be critical for neuronal coding, for example, by reducing pair-wise spike train correlations and reducing redundancy across populations of neurons, perhaps in conjunction with connectivity^{7,8}. Such decreases would afford populations of highly diverse neurons additional bandwidth with which to code for stimuli, as has been suggested by theoretical studies^{9,10}. In noisy neural systems, where trial-to-trial variability is large¹¹, the manner in which redundancy and bandwidth are balanced remains unexplored. At one extreme, biophysical differences may simply be the product of the imprecision of biology. For example, mosaics of neuronal properties may only reflect the probabilistic nature of gene expression among different cells. Alternatively, this diversity may be a functionally important adaptation in which the noise of stochastic gene expression is harnessed in the service of neuronal coding. Thus, understanding the effects of intrinsic diversity on neural responses and neuronal coding is essential for linking the cell biology of neurons with their function in information coding in the context of neuronal circuits. Heterogeneity in responses can arise from numerous sources, including anatomical differences and differences in inputs. We focused on the mitral cells of the main olfactory

bulb, where input correlations in mitral cells connected to the same glomerulus are high¹² and the anatomy is highly stereotypic.

We found that intrinsic biophysical diversity affects neuronal coding by reducing correlations in the population code while simultaneously increasing the information encoded by the population. The coding capacity of populations of biophysically heterogeneous cells was twofold higher than that of their homogeneous counterparts. This enhancement was seen for both random noisy inputs and physiologically relevant stimuli modulated by oscillations corresponding to the frequency of sniffing. In addition, we found that the spike-triggered average (STA) could be used to quantify neuronal diversity. Our data imply that biophysical heterogeneity is an important mechanism of robust population coding rather than an unavoidable consequence of biology's imprecision.

RESULTS

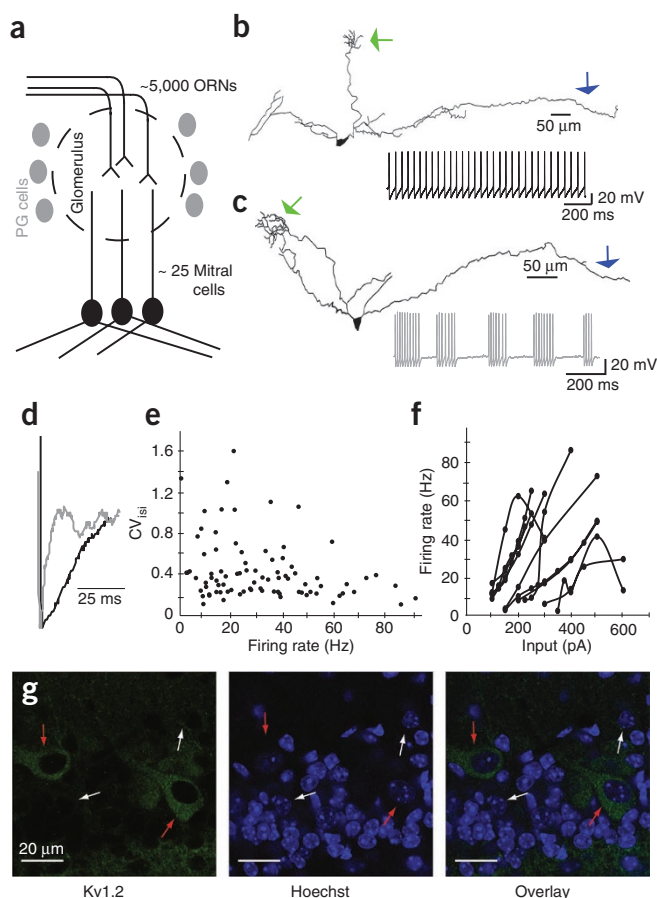
Mitral cells have intrinsic biophysical diversity

To understand the role of intrinsic diversity in neuronal coding, we made recordings from mitral cells of the mouse main olfactory bulb *in vitro* (Fig. 1a). In the olfactory bulb, groups of ~25 mitral cells receive their excitatory input from the same population of several thousand olfactory receptor neurons (ORNs) in structures known as glomeruli¹³. Each glomerulus is the convergence point of all ORN axons expressing the same odorant receptor that together provide highly correlated inputs to mitral cells (Fig. 1a)^{13,14}. Mitral cells activated by the same odor in the same animal have different temporal responses^{8,15,16}. In most cases, these responses are the result of responses from mitral cells connected to different glomeruli⁸. However, highly variable responses have been observed even when cells are connected to the same glomerulus¹⁷, suggesting that strongly correlated inputs only trigger weakly correlated outputs, not unlike what has been reported in neocortex^{7,18}. To explore differences in mitral cell intrinsic properties, we first injected a constant direct

¹Department of Biological Sciences, Carnegie Mellon University, Pittsburgh, Pennsylvania, USA. ²Center for the Neural Basis of Cognition, Pittsburgh, Pennsylvania, USA. ³Department of Neuroscience, University of Pittsburgh, Pittsburgh, Pennsylvania, USA. Correspondence should be addressed to N.N.U. (nurban@cmu.edu).

Received 28 June; accepted 28 July; published online 29 August 2010; doi:10.1038/nn.2630

Figure 1 Intrinsic diversity of mitral cell populations. **(a)** Schematic of mammalian main olfactory bulb circuitry. ORNs expressing one olfactory receptor all send their axons to the same glomerulus. All mitral/tufted cell apical dendrites connected to a glomerulus receive inputs that are highly correlated. **(b,c)** Biocytin fills of two representative mitral cells with spike responses to a fixed direct current. In both cells, apical dendrites and their tufts (green arrow) and lateral dendrites (blue arrow) were intact in the slice. **(d)** Mitral cell spike outputs were also diverse on the basis of the shape of the after hyperpolarizations that follow their action potentials (color corresponds to traces in **b** and **c**). **(e)** Mitral cells differ widely in both firing rates and in the coefficients of variation of their interspike intervals (CV_{isi}). **(f)** Recordings of mitral cells showed wide variation in excitability as described by the frequency of action potentials generated by constant current stimuli of different amplitudes. **(g)** Confocal micrographs of the olfactory bulb stained for Kv1.2 (green) and Hoechst (blue). An overlaid image, Kv1.2-positive cell bodies and mitral cell nuclei, is shown on the right. Red arrows highlight cell bodies of Kv1.2-positive neurons and their nuclei and white arrows highlight nuclei of mitral cells that did not express Kv1.2. Kv1.2-positive and Kv1.2-negative mitral cells are interspersed in the same focal plane.



current into the mitral cell soma. This stimulus produced marked variability in mitral cell output spike patterns ($n = 34$ cells, 19 animals; **Fig. 1b,c**). This variability was preserved in cells in which apical dendrites and lateral dendrites were intact, suggesting that spike pattern differences were not a result of differences in morphology or of artifacts in slicing ($n = 8$). Analysis of these reconstructed mitral cells revealed that they all had both apical and lateral dendrites (eight of eight), 75% of cells (six of eight) had well ramified apical tufts, and 62.5% (five of eight) had multiple obvious lateral dendrites extending throughout the bulb slice. The total length of reconstructed dendritic processes was $1,860 \pm 494 \mu\text{m}$ ($n = 8$). Thus, although the cells were anatomically similar, they differed markedly in their firing patterns, including in the spike after-hyperpolarization (**Fig. 1d**).

Even neurons firing at similar rates (**Fig. 1b,c**) fired more or less regularly, as measured by the coefficient of variation of their interspike intervals (CV_{isi} , 0.09 and 1.12; **Fig. 1b,c**). This was typical of the variability seen across all of the mitral cells that we recorded (ISI coefficient of variation = 0.44 ± 0.33 ; **Fig. 1e**) and was indicative of the physiological signatures of their intrinsic biophysical differences^{19,20}. Furthermore, mitral cells had highly variable input-output functions (firing rate to a given direct current input, $n = 11$ cells; **Fig. 1f**).

Differential expression of voltage-gated ion channels can lead to differences in intrinsic properties⁶. To characterize this differential channel expression, we immunostained mitral cell populations for one subunit of the voltage-gated potassium channel Kv1.2 (**Fig. 1g**). Kv1.2-positive mitral cells were right next to cells that were Kv1.2 negative (**Fig. 1g**), suggesting that one source of intrinsic diversity in the mitral cell population is the differential expression of the Kv1.2 subunit.

Mitral cell responses to complex stimuli are cell specific

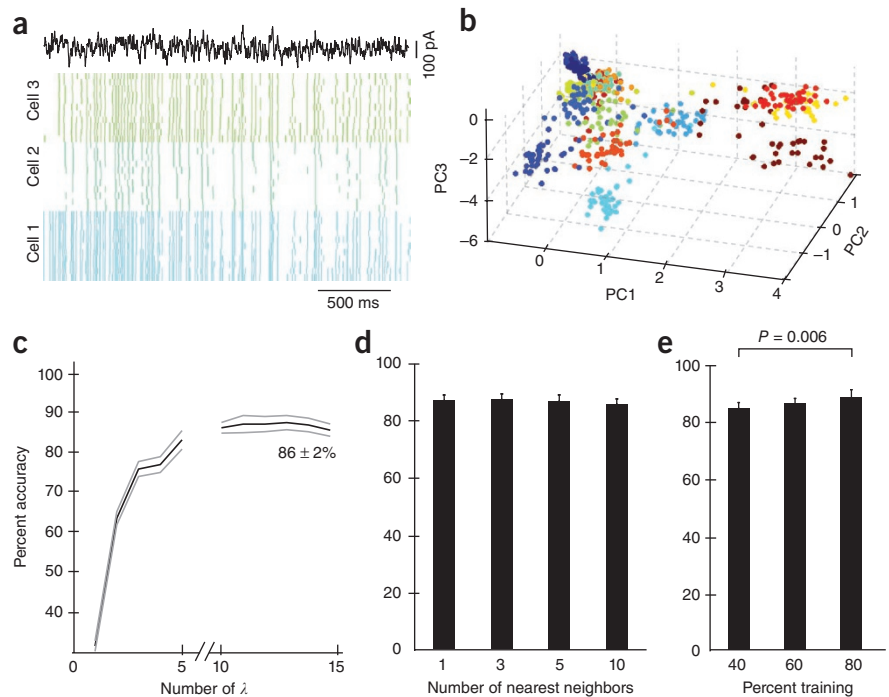
Fixed direct current injection, as used above to identify regular spiking versus bursting mitral cells (**Fig. 1b,c**), fail to capture the complex dynamics of neuronal firing²¹. To understand the effects of intrinsic diversity on neuronal output, we recorded mitral cell responses (in ACSF, containing 25 μM D(-)-2-amino-5-phosphonovaleric acid (AP5), 10 μM 6-cyano-7-nitroquinoxaline-2,3-dione (CNQX) and 10 μM bicuculline to block fast synaptic transmission and isolate intrinsic properties) to identical rapidly fluctuating currents (filtered Gaussian white noise, $\sigma = 40$ pA, direct current = 100–400 pA, $n = 15$ over multiple trials (30–40 trials); **Fig. 2a**, **Supplementary Analysis** and **Supplementary Fig. 1**). As all synaptic transmission was blocked, differences in spike output were the result of intrinsic biophysical

variability. Identical experiments performed without blocking synaptic transmission yielded similar results, indicating that these differences were also present under different physiological conditions (data not shown).

Identical input noise triggered reliable spike trains in a single cell^{22,23}, but the spike trains in different mitral cells varied considerably (**Fig. 2a**). To classify this output diversity, we carried out principal component analysis (**Supplementary Fig. 2**) on the spike trains. As there were no slow covarying elements in the first three principal components (**Supplementary Fig. 2**), each cell's response reflected a differential filtering of the rapidly fluctuating current in the stimulus, rather than slow decorrelation or spike-frequency adaptation. Projecting each spike train onto the first three principal components (**Fig. 2b**) showed that, although the across-cell responses were broadly distributed, within-cell responses were tightly packed.

To measure the similarities and the differences of spike trains within and between mitral cells in this space, we classified each of the trials from the different recorded cells to the stimulus using the K nearest neighbor algorithm. Using only the first 15 principal components (three nearest neighbors, using 60% of data for training), spike trains could be correctly classified as originating from a particular neuron with $86 \pm 2\%$ accuracy (**Fig. 2c**). Furthermore, the number of nearest neighbors (**Fig. 2d**), ranging from one to ten, did not affect classification accuracy (one nearest neighbor = $86.7 \pm 2\%$, ten nearest neighbors = $85.5 \pm 2\%$, $P = 0.07$, ANOVA) when 60% of the trials were used, suggesting that the clustering of spike responses was tight. Thus, a spike train from a single cell was more similar to the other spike trains from that cell than to spike trains from other cells. When changing the percentage of training versus testing data, a small

Figure 2 Uniqueness of mitral cell output to identical input. (a) Spike rasters of ten trials for three mitral cells to an identical fluctuating input (black trace). (b) Projection of all spike patterns (points) from multiple cells (colors) onto a space defined by the first three principal components (PC1, PC2 and PC3) calculated from all spike trains. (c) Classification accuracy of spike trains on the basis of recording identity as a function of the number of eigenvectors (λ) used for classification. (d) The number of nearest neighbors (1, 3, 5 and 10) did not affect the classification accuracy. (e) The percentage of trials used in the testing and the training sets affected the classification accuracy only when 80% of spike trains were used in training. Error bars represent s.d.



effect on classification accuracy was observed (40% testing data gave $85 \pm 3\%$, training accuracy, 80% testing data gave $88.8 \pm 3\%$ accuracy, $P = 0.006$, ANOVA; **Fig. 2e**). Thus, the responses of all of the trials in a single condition were highly reproducible and classification accuracy decreased only nominally when the number of trials used for training was halved. Consequently, spike trains to the identical stimulus were reliable across trials in one cell, but specific across all cells.

Intrinsic diversity reduces correlations in spike output

Correlated spiking can emerge as a result of reliable firing among populations of cells that are driven by inputs that are highly correlated¹⁷. However, intrinsic diversity may reduce pair-wise correlations between cells. To explore this question, we calculated the correlations of spike trains across all trials in the same cell and between trials in different mitral cells to this identical input (**Supplementary Fig. 3**). Spike train correlations across trials recorded from a single cell were high, but were much lower between the trials of different cells (within cell $R^2 = 0.17 \pm 0.002$, between cell $R^2 = 0.04 \pm 0.00$, $n = 15$, $P = 3.7 \times 10^{-10}$; **Fig. 3a**). When pair-wise correlations across all trials from all cells to the stimulus were compared ($n = 589$ trials, 30–40 trials per condition), the mean was $R^2 = 0.08 \pm 0.09$ (1-ms window, **Fig. 3b**).

Thus, the intrinsic differences between this population of mitral cells reduce correlations of mitral cell responses to fluctuating inputs. The pair-wise similarity between spike trains was low even when the inputs that drove those spikes were perfectly correlated. Low output correlations were not exclusively the result of differences in firing rate;

near-zero correlations were observed even with similar firing rates (**Fig. 3c**). Furthermore, when the precision by which correlation was measured was relaxed, pair-wise population correlations were still only 0.34 ± 0.15 for a 16-ms window (**Supplementary Fig. 3**). Thus, intrinsic diversity between mitral cells alone was sufficient to reduce correlations between neural spike trains.

Diversity can be described by analysis of STAs

Rapidly fluctuating stimuli²¹, in addition to providing an input for assessing correlation²³, can be used to probe the complex features of a cell's intrinsic dynamics²⁴. To explore this further^{11,22,23,25}, we injected a family of rapidly fluctuating currents that differed in their variance and direct current offset ($\sigma = 20$ –80 pA, direct current = 100–600 pA; **Supplementary Fig. 1**) into a population of recorded mitral cells in which all excitatory and inhibitory synapses were blocked (25 μ M AP5, 10 μ M CNQX, 10 μ M bicuculline). In addition, identical experiments were performed where synaptic activity remained and yielded similar results. To characterize the features of the stimulus to which each neuron responded, we calculated the average stimulus waveform preceding all the spikes in that neuron, the STA (**Supplementary Figs. 4 and 5**)^{24,26,27}, for each cell. Differences in STAs indicated that different mitral cells were filtering different features of the stimulus and the different filters reflected differences in the biophysical properties of these neurons²⁴. The STAs of several example cells (**Fig. 2a**) were highly variable (**Fig. 4a**), representative of the heterogeneity in stimulus filters across all of the mitral cells that were recorded ($n = 35$ STAs; **Fig. 4b**).

To analyze these filters, we carried out principal component analysis on the STAs (**Supplementary Fig. 4**), allowing each STA to be represented as a linear combination of principal components²⁸. The first three components (**Fig. 4c**) accounted for 90%

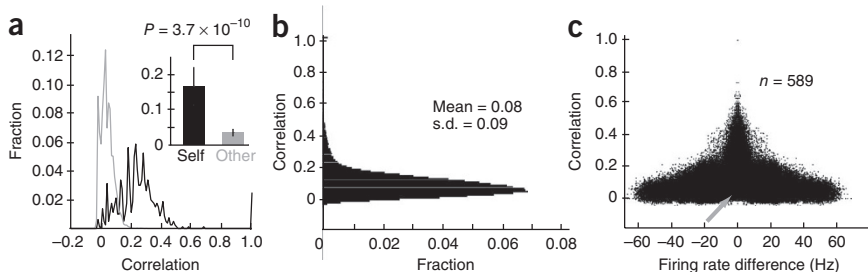


Figure 3 Intrinsic diversity affects pair-wise spike train correlations. (a) Histogram of all pair-wise correlations for within-cell (black) and between-cell spike trains (gray). Inset, mean pair-wise correlations were significantly different for within cells and between cells. (b) Histogram of all pair-wise correlations from cells receiving an identical input. (c) Pair-wise correlations of all spike trains from all mitral cells as a function of differences in firing rates. Error bars represent s.d.

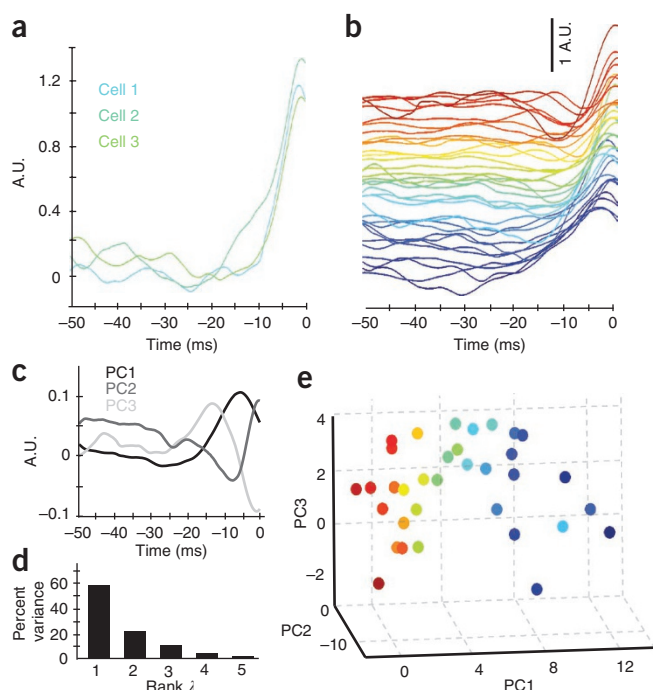


Figure 4 Mitral cell STA diversity. (a) STAs for the three cells shown in **Figure 3a**. (b) STAs for a population of mitral cells that all received noisy input illustrates the diversity ($n = 35$ STAs). Color corresponds to identity in **e**. (c) Principal components (PC1, PC2 and PC3) of the STAs shown in **b**. (d) Variance explained by the first five principal components for this population of mitral cells. (e) Projection of each STA onto the space of principal components in **c** indicated that mitral cell STAs were not uniformly distributed, but spanned an arc in the space.

of the STA variance (**Fig. 4d**) and their projection into the space defined by these components (**Fig. 4e**) indicated that STAs were not uniformly distributed and that diversity was preserved across multiple firing rates (**Supplementary Figs. 4 and 5**). Consequently, STA shapes projected onto the space defined by the first three principal components allowed us to visualize the distribution of intrinsic biophysical variability.

Biophysical diversity predicts information gain

To connect intrinsic diversity (STA) to information coding, we evoked spike trains in many neurons at different direct current values ($n = 15$) using a rapidly fluctuating identical stimulus^{21,23} over multiple trials ($m = 30$ – 70 trials per cell, six representative trials; **Fig. 5a** and **Supplementary Fig. 1**). This can be seen as being analogous to the case in which groups of mitral cells receive highly similar inputs from the same population of sensory receptor neurons¹⁴. As all mitral cells received identical input fluctuations and all synaptic activity was blocked, differences in spike output were the result of intrinsic biophysical diversity. From these recordings, we generated homogeneous ($n = 45$ populations per network size) and heterogeneous populations ($n = 200$ populations per network size) ranging in size from two to ten mitral cells to explore the connection between diversity and entropy/information in spike output (**Fig. 5b** and **Supplementary Fig. 6**)⁹. We generated homogeneous population responses by drawing spike trains from the set of trials recorded in a single neuron (**Fig. 5b**), equivalent to the case in which a stimulus was encoded by identical cells receiving the same input. In contrast, heterogeneous responses were created by randomly selecting groups of non-identical neurons from the population of all recorded cells (**Fig. 5b**). Spike trains recorded on individual trials for each of these different cells (**Fig. 5b**) were then drawn randomly to create the heterogeneous response (**Fig. 5b**), analogous to a case in which biophysically distinct cells process the same input ($N = 2,000$ trials per network; **Supplementary Fig. 7**)²⁹. When the number of neurons in the population was small (for example, two cells; **Fig. 5c**), only small differences between the information transmitted by the homogeneous

population (0.60 ± 0.15 bits per 8-ms bin) and the heterogeneous population (0.71 ± 0.12 bits per 8-ms bin) could be identified. However, as the population size grew, heterogeneous networks quickly carried more information than their homogeneous counterparts (**Fig. 5c**). Gains increased by up to 2.1-fold (**Fig. 5c** and **Supplementary Fig. 7**) in the largest network examined (ten mitral cells), in which heterogeneous populations carried 2.66 ± 0.12 bits per 8 ms, which was significantly more than homogeneous populations of the same size (1.27 ± 0.07 bits per 8 ms, $P < 5 \times 10^{-7}$, ANOVA).

To determine whether biophysical diversity accounted for the increases in information, we related the population's STA diversity to the information it encodes about the stimulus for each set of heterogeneous mitral cells ($n = 1,800$ different simulated populations; **Fig. 6**). We used the STAs of example neurons (**Fig. 6a**) as a measure of that mitral cell's intrinsic diversity contribution to the population (**Fig. 6b**). From this, pair-wise distances between these STAs (**Fig. 6c**) in the principal component space (**Fig. 4**) could be calculated. As the mitral cell population's STA diversity increased, the bits of stimulus information relayed by those populations continued to increase to 2.60 ± 0.16 bits per 8 ms ($R^2 = 0.89$, $n = 1,800$; **Fig. 6d**). Thus, the more intrinsically diverse the population, the more information that the ensemble of mitral cells conveyed (**Fig. 6d** and **Supplementary Figs. 8 and 9**).

Diversity increases information during oscillatory inputs

In mammals, inputs to mitral cells are strongly modulated by oscillatory drive, corresponding to the animal's sniffing cycle (1–10 Hz in mice), and this periodic sampling of odors is thought to be essential

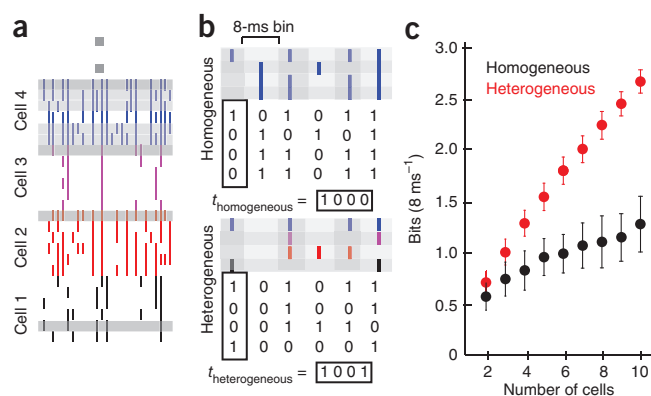


Figure 5 Heterogeneous populations of mitral cells carry more information than their homogeneous counterparts. (a) Representative trials of spike trains (six per cell) from four mitral cells all given an identical fluctuating input. (b) A homogeneous population response was constructed by randomly drawing spike trains from a single recorded cell (blue). A heterogeneous population was constructed by randomly drawing spike trains from different neurons. The responses of each population were binarized into words of 0s and 1s and the pattern of words (for instance, $t_{\text{homogeneous}}$ and $t_{\text{heterogeneous}}$) was analyzed to calculate information. (c) Heterogeneous populations of mitral cells carry twice as much information as homogeneous populations of cells. Error bars represent s.d.

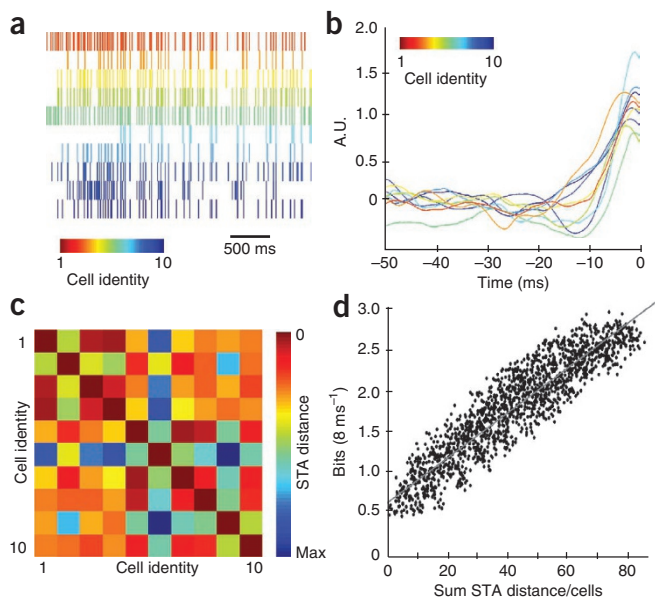
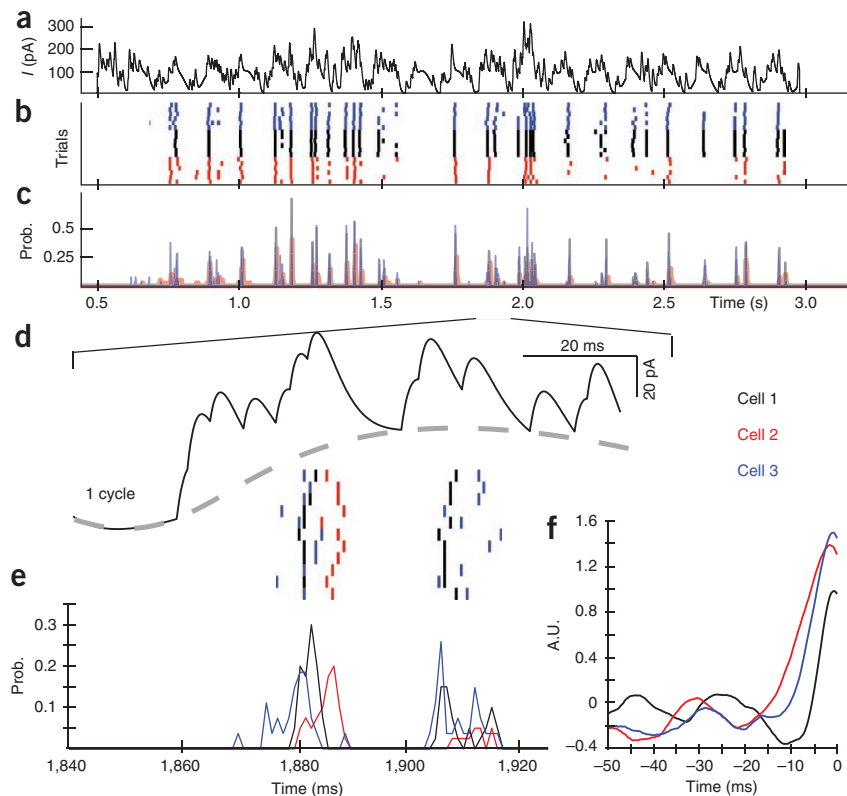


Figure 6 Biophysical diversity correlates to information transfer. (a) Spike train examples of a single trial for ten mitral cells with different STAs. (b) STAs of the ten cells in **a** color coded by cell identity. (c) STA distance matrix calculated by measuring the Euclidian distance of the STAs to one another in the space defined by the principal components. (d) Bits of information as a function of the sum of STA distance divided by the number of cells.

for behavior and the processing of odor information^{30,31}. To determine whether the gain in information conferred by biophysically heterogeneous was present when mitral cells received physiologically relevant stimuli, we injected mitral cells with both synaptic barrages generated by convolving a random spike train with an alpha function and synaptic barrages modulated with an underlying 8-Hz oscillation ($n = 11$ cells with theta, 23 cells total). Spike trains from mitral cells ($n = 27$ –40 spike trains per cell; **Fig. 7a** and **Supplementary Fig. 10**) presented with an identical synaptic barrage or a synaptic barrage and an 8-Hz current were collected over multiple trials in both of these conditions. Again, these two conditions could be thought of as the case in which populations of mitral cells receive highly similar synaptic inputs modulated by sniffing from groups of sensory neurons expressing the same olfactory receptor proteins. We examined the responses of individual mitral cells (**Fig. 7b**), along with the

Figure 7 Heterogeneous populations improve the coding of physiologically relevant stimuli. (a) Synaptic input currents modulated by an 8-Hz periodic oscillation. (b) Responses of six trials each from three mitral cells to the identical periodic input. (c) Probability of spike firing at various stimulus epochs. (d) Enlargement of one theta cycle and spike times for the three cells in **b** over multiple trials. (e) Probability of firing during the cycle. (f) STAs for the three mitral cells calculated by injecting a rapidly fluctuating noisy input.



probability of spiking throughout the stimulus of each of cell (**Fig. 7c**). The underlying theta rhythm resulted in locking of spike patterns to specific phases of the oscillation³², notably to the rising phase and the peak (**Fig. 7c**). However, when the precise timing of spikes in these cells was examined, differences quickly became apparent (**Fig. 7d,e**). Specifically, even mitral cells firing at similar rates (11.5 ± 1.9 , 8.6 ± 2.1 and 13.7 ± 1 Hz) showed considerable heterogeneity with spike times for each neuron staggered throughout various phases of the oscillation (**Fig. 7d**). When the STAs of these different mitral cells were calculated by injecting a noisy stimulus (**Fig. 7f**), they were indeed different. Thus the STA, in addition to reflecting each neuron's unique biophysical fingerprint, also reflects the diversity of that neuron's spike timing across various phases of an input driven by strong theta oscillatory activity.

To determine the extent to which these differences in spike timing across theta cycles allowed mitral cells to code for information, we created model populations of homogeneous and heterogeneous neurons as before (**Fig. 6a**) from cells that all received the same synaptic input and the same synaptic input modulated by a theta oscillation. For synaptic inputs, eight cell heterogeneous populations ($n = 100$) carried 1.67 ± 0.13 bits per 8 ms, significantly more ($P = 1.3 \times 10^{-30}$, ANOVA) than their eight cell homogeneous network ($n = 11$) counterparts, which carried only 0.91 ± 0.3 bits per 8 ms). Eight cell heterogeneous networks ($n = 100$) that received synaptic inputs that rode on top of an underlying 8-Hz oscillation carried 24.5 ± 2.5 bits per sniff, significantly more ($P = 5.1 \times 10^{-24}$, ANOVA) than the information carried by eight cell homogeneous networks (12.6 ± 5.8 bits per sniff, $n = 11$). Taken together, these data suggest that biophysically heterogeneous populations of mitral cells can code for up to 1.9-fold more information per sniff cycle than biophysically homogeneous populations of mitral cells. Furthermore, the degree of biophysical heterogeneity as measured by STA diversity correlated with the gains

in information across different types of physiologically relevant stimuli (Supplementary Fig. 10). Therefore, the coding capacity gains associated with diverse populations of mitral cells appeared to be preserved across a host of conditions, ranging from noisy stimuli to synaptic inputs modulated by a strong 8-Hz oscillation. In sum, the computational advantages conferred by intrinsic biophysical heterogeneity are a general feature of neural coding across a range of physiologically relevant stimuli.

DISCUSSION

Intrinsic diversity's role in correlation and coding

Although neurons have long been known to be diverse in their anatomical and physiological properties^{3,33}, our results are, to the best of our knowledge, the first to demonstrate the importance of intrinsic biophysical diversity in a population of neurons (mitral cells of the olfactory bulb) that are believed to be highly homogeneous and have been shown to receive highly correlated inputs¹⁴. A neuron's response to incoming stimuli is shaped by the voltage-gated ion channels expressed in that cell^{34,35}. Different combinations of these channels may generate functional differences or may result in a population of neurons that are physiologically similar despite being molecularly different^{6,36}. Consequently, the diversity that emerges from individual differences in gene expression³⁷ in some cases appears to be nullified by the combinatorial expression of different channels in that cell. In such instances, intrinsic diversity is titrated to produce equivalent output responses⁶. In other cases, populations of inhibitory³ and excitatory^{33,38} neurons in both the mammalian neocortex and inhibitory neurons in the *Drosophila* olfactory system³⁹ exhibit a notable intrinsic diversity. In these regions and populations of neurons, differences in the expression of ion channels and morphology result in the marked heterogeneity of the intrinsic properties of those cells³⁹ and the responses are therefore diverse even when similar inputs are delivered³³. Although a number of mechanisms have been proposed to account for the origin and extent of these intrinsic differences⁴⁰, we found that differences in intrinsic biophysical heterogeneity can be important neural coding.

One aspect of coding in which heterogeneity may be important is in correlated activity among populations of cells⁴¹. Correlations in output spiking can occur as a result of cells receiving highly correlated inputs¹², but these output correlations are often substantially less than the input correlations¹⁷ as a result of a number of factors⁸, including active decorrelation resulting from network connections^{7,42}. Although the degree and origin¹⁷ of this correlated firing remains controversial^{7,18}, our results indicate that intrinsic diversity alone is sufficient to erode output correlations even when inputs are shared and when only a single population of neurons is considered. Precise correlations have been identified as being crucial in a number of systems, including the olfactory bulb⁴³. In the antenna lobe, the insect analog of the mammalian olfactory system, spiking activity is synchronized by 20-Hz oscillations⁴⁴ and desynchronization of this activity degrades the odor representation and impairs discrimination⁴⁵. Our results also suggest that intrinsic biophysical diversity among mitral cells may reduce the degree to which firing is correlated even when incoming ORN excitatory inputs are very similar and gated by oscillatory drive. In mammals, where respiratory drive and sniffing produce strong oscillatory input in the theta frequency, diverse cells may exploit their intrinsic differences to spread spikes across various phases of the underlying respiratory cycle, improving the information coding capacity of the population, as we found here.

Diversity of intrinsic properties may also influence the extent to which mitral cells can be synchronized by aperiodic inhibition⁴⁶.

Reciprocal interactions between mitral cells and the inhibitory population of granule cells to which they are connected may be an additional source of diversity that can dynamically⁴² alter the correlational structure of the spike outputs⁴⁷. In this respect, important relationships could exist between the dynamics of individually heterogeneous cells and the networks in which they are embedded.

Among the many approaches taken to examine questions of neural computation, biophysical models of single neurons and statistical analysis of populations of neurons have both been powerful. Dynamical systems approaches have provided insight into how single neurons and networks respond to stimuli¹¹. Simultaneously, the statistical characterization of neuronal responses and neuronal variability has allowed neural computation to be described in terms of the functions being performed^{21,29}. Largely absent, however, is a framework that relates diversity in the parameters for spike generation in a single neuron with the coding of a population of neurons comprised of these diverse individual cells. Building on our previous work²⁴ showing how the STA, a concept in neural coding, is related to the phase resetting curve (PRC), an idea from neuronal dynamics, we investigated how diversity at the single cell STA level (and, by extension, the single cell PRC) contributes to efficient population coding. Our data establish a bridge linking these two frameworks, connecting the dynamical systems perspective (PRC→STA) of a single neuron with the statistical perspective of a population code (STA→bits). Thus, population coding may not simply be the product of more neurons or more connections, but instead depends on the contributions of intrinsic biophysical diversity to tie these elements together.

METHODS

Methods and any associated references are available in the online version of the paper at <http://www.nature.com/natureneuroscience/>.

Note: Supplementary information is available on the Nature Neuroscience website.

ACKNOWLEDGMENTS

We wish to thank G.M. LaRocca for assistance with the immunohistochemistry and B. Benedetti, A. Barth, J. Castro and members of the Urban laboratory for helpful comments on this manuscript. Funding was provided by the National Institute on Deafness and Other Communication Disorders (R01DC0005798).

AUTHOR CONTRIBUTIONS

K.P. conducted the experiments and the analysis. K.P. and N.N.U. wrote the manuscript.

COMPETING FINANCIAL INTERESTS

The authors declare no competing financial interests.

Published online at <http://www.nature.com/natureneuroscience/>.

Reprints and permissions information is available online at <http://www.nature.com/reprintsandpermissions/>.

- Ramón y Cajal, S. Structure and connections of neurons. *Bull. Los Angel. Neuro. Soc.* **17**, 5–46 (1952).
- Marder, E. & Goaillard, J.M. Variability, compensation and homeostasis in neuron and network function. *Nat. Rev. Neurosci.* **7**, 563–574 (2006).
- Gupta, A., Wang, Y. & Markram, H. Organizing principles for a diversity of GABAergic interneurons and synapses in the neocortex. *Science* **287**, 273–278 (2000).
- Mainen, Z.F. & Sejnowski, T.J. Influence of dendritic structure on firing pattern in model neocortical neurons. *Nature* **382**, 363–366 (1996).
- Schaefer, A.T., Larkum, M.E., Sakmann, B. & Roth, A. Coincidence detection in pyramidal neurons is tuned by their dendritic branching pattern. *J. Neurophysiol.* **89**, 3143–3154 (2003).
- Schulz, D.J., Goaillard, J.M. & Marder, E. Variable channel expression in identified single and electrically coupled neurons in different animals. *Nat. Neurosci.* **9**, 356–362 (2006).
- Ecker, A.S. *et al.* Decorrelated neuronal firing in cortical microcircuits. *Science* **327**, 584–587 (2010).
- Friedrich, R.W. & Laurent, G. Dynamic optimization of odor representations by slow temporal patterning of mitral cell activity. *Science* **291**, 889–894 (2001).

9. Stocks, N.G. Suprathreshold stochastic resonance in multilevel threshold systems. *Phys. Rev. Lett.* **84**, 2310–2313 (2000).
10. Brody, C.D. & Hopfield, J.J. Simple networks for spike timing-based computation, with application to olfactory processing. *Neuron* **37**, 843–852 (2003).
11. Ermentrout, G.B., Galan, R.F. & Urban, N.N. Reliability, synchrony and noise. *Trends Neurosci.* **31**, 428–434 (2008).
12. Chen, T.W., Lin, B.J. & Schild, D. Odor coding by modules of coherent mitral/tufted cells in the vertebrate olfactory bulb. *Proc. Natl. Acad. Sci. USA* **106**, 2401–2406 (2009).
13. Mombaerts, P. *et al.* Visualizing an olfactory sensory map. *Cell* **87**, 675–686 (1996).
14. Wachowiak, M., Denk, W. & Friedrich, R.W. Functional organization of sensory input to the olfactory bulb glomerulus analyzed by two-photon calcium imaging. *Proc. Natl. Acad. Sci. USA* **101**, 9097–9102 (2004).
15. Wellis, D.P., Scott, J.W. & Harrison, T.A. Discrimination among odorants by single neurons of the rat olfactory bulb. *J. Neurophysiol.* **61**, 1161–1177 (1989).
16. Margrie, T.W., Sakmann, B. & Urban, N.N. Action potential propagation in mitral cell lateral dendrites is decremental and controls recurrent and lateral inhibition in the mammalian olfactory bulb. *Proc. Natl. Acad. Sci. USA* **98**, 319–324 (2001).
17. Kazama, H. & Wilson, R.I. Origins of correlated activity in an olfactory circuit. *Nat. Neurosci.* **12**, 1136–1144 (2009).
18. Renart, A. *et al.* The asynchronous state in cortical circuits. *Science* **327**, 587–590 (2010).
19. Schoppa, N.E. & Westbrook, G.L. Regulation of synaptic timing in the olfactory bulb by an A-type potassium current. *Nat. Neurosci.* **2**, 1106–1113 (1999).
20. Chen, W.R. & Shepherd, G.M. Membrane and synaptic properties of mitral cells in slices of rat olfactory bulb. *Brain Res.* **745**, 189–196 (1997).
21. de Ruyter van Steveninck, R.R., Lewen, G.D., Strong, S.P., Koberle, R. & Bialek, W. Reproducibility and variability in neural spike trains. *Science* **275**, 1805–1808 (1997).
22. Mainen, Z.F. & Sejnowski, T.J. Reliability of spike timing in neocortical neurons. *Science* **268**, 1503–1506 (1995).
23. Galán, R.F., Ermentrout, G.B. & Urban, N.N. Optimal time scale for spike-time reliability: theory, simulations and experiments. *J. Neurophysiol.* **99**, 277–283 (2008).
24. Ermentrout, G.B., Galan, R.F. & Urban, N.N. Relating neural dynamics to neural coding. *Phys. Rev. Lett.* **99**, 248103 (2007).
25. Bryant, H.L. & Segundo, J.P. Spike initiation by transmembrane current: a white-noise analysis. *J. Physiol. (Lond.)* **260**, 279–314 (1976).
26. Schwartz, O., Pillow, J.W., Rust, N.C. & Simoncelli, E.P. Spike-triggered neural characterization. *J. Vis.* **6**, 484–507 (2006).
27. Meister, M., Pine, J. & Baylor, D.A. Multi-neuronal signals from the retina: acquisition and analysis. *J. Neurosci. Methods* **51**, 95–106 (1994).
28. Geffen, M.N., Broome, B.M., Laurent, G. & Meister, M. Neural encoding of rapidly fluctuating odors. *Neuron* **61**, 570–586 (2009).
29. Osborne, L.C., Palmer, S.E., Lisberger, S.G. & Bialek, W. The neural basis for combinatorial coding in a cortical population response. *J. Neurosci.* **28**, 13522–13531 (2008).
30. Wesson, D.W., Verhagen, J.V. & Wachowiak, M. Why sniff fast? The relationship between sniff frequency, odor discrimination and receptor neuron activation in the rat. *J. Neurophysiol.* **101**, 1089–1102 (2009).
31. Verhagen, J.V., Wesson, D.W., Netoff, T.I., White, J.A. & Wachowiak, M. Sniffing controls an adaptive filter of sensory input to the olfactory bulb. *Nat. Neurosci.* **10**, 631–639 (2007).
32. Schaefer, A.T., Angelo, K., Spors, H. & Margrie, T.W. Neuronal oscillations enhance stimulus discrimination by ensuring action potential precision. *PLoS Biol.* **4**, e163 (2006).
33. Wang, Y. *et al.* Heterogeneity in the pyramidal network of the medial prefrontal cortex. *Nat. Neurosci.* **9**, 534–542 (2006).
34. Day, M. *et al.* Dendritic excitability of mouse frontal cortex pyramidal neurons is shaped by the interaction among HCN, Kir2 and K_{leak} channels. *J. Neurosci.* **25**, 8776–8787 (2005).
35. Taylor, A.L., Goaillard, J.M. & Marder, E. How multiple conductances determine electrophysiological properties in a multicompartment model. *J. Neurosci.* **29**, 5573–5586 (2009).
36. Goaillard, J.M., Taylor, A.L., Schulz, D.J. & Marder, E. Functional consequences of animal-to-animal variation in circuit parameters. *Nat. Neurosci.* **12**, 1424–1430 (2009).
37. Sugino, K. *et al.* Molecular taxonomy of major neuronal classes in the adult mouse forebrain. *Nat. Neurosci.* **9**, 99–107 (2006).
38. Wang, Y., Gupta, A., Toledo-Rodriguez, M., Wu, C.Z. & Markram, H. Anatomical, physiological, molecular and circuit properties of nest basket cells in the developing somatosensory cortex. *Cereb. Cortex* **12**, 395–410 (2002).
39. Chou, Y.H. *et al.* Diversity and wiring variability of olfactory local interneurons in the *Drosophila* antennal lobe. *Nat. Neurosci.* **13**, 439–449 (2010).
40. Desai, N.S., Rutherford, L.C. & Turrigiano, G.G. Plasticity in the intrinsic excitability of cortical pyramidal neurons. *Nat. Neurosci.* **2**, 515–520 (1999).
41. Salinas, E. & Sejnowski, T.J. Correlated neuronal activity and the flow of neural information. *Nat. Rev. Neurosci.* **2**, 539–550 (2001).
42. Arevian, A.C., Kapoor, V. & Urban, N.N. Activity-dependent gating of lateral inhibition in the mouse olfactory bulb. *Nat. Neurosci.* **11**, 80–87 (2008).
43. Laurent, G. *et al.* Odor encoding as an active, dynamical process: experiments, computation and theory. *Annu. Rev. Neurosci.* **24**, 263–297 (2001).
44. Bazhenov, M. *et al.* Model of transient oscillatory synchronization in the locust antennal lobe. *Neuron* **30**, 553–567 (2001).
45. Stopfer, M., Bhagavan, S., Smith, B.H. & Laurent, G. Impaired odour discrimination on desynchronization of odour-encoding neural assemblies. *Nature* **390**, 70–74 (1997).
46. Galán, R.F., Fourcaud-Trocmé, N., Ermentrout, G.B. & Urban, N.N. Correlation-induced synchronization of oscillations in olfactory bulb neurons. *J. Neurosci.* **26**, 3646–3655 (2006).
47. Kashiwadani, H., Sasaki, Y.F., Uchida, N. & Mori, K. Synchronized oscillatory discharges of mitral/tufted cells with different molecular receptive ranges in the rabbit olfactory bulb. *J. Neurophysiol.* **82**, 1786–1792 (1999).

ONLINE METHODS

Animal procedures. All procedures were carried out in accordance with the guidelines for the care and use of animals at Carnegie Mellon University (Institutional Animal Care and Use Committee of Carnegie Mellon University) and as previously described^{48,49}. Briefly, C57Bl/6 mice between postnatal days 11 and 19 (P11 and P19) were deeply anesthetized with isoflurane and then decapitated. Brains were removed and placed in ice-cold Ringer's solution (125 mM NaCl, 25 mM glucose, 2.5 mM KCl, 25 mM NaHCO₃, 1.25 mM NaH₂PO₄, 1 mM MgCl₂ and 2.5 mM CaCl₂). We made 300- μ m-thick coronal sections from the main olfactory bulb using a vibratome (VT1000S, Leica). After cutting, slices were incubated in Ringer's solution of (125 mM NaCl, 25 mM glucose, 2.5 mM KCl, 25 mM NaHCO₃, 1.25 mM NaH₂PO₄, 1 mM MgCl₂ and 2.5 mM CaCl₂) at 37 °C for 30 min before recordings were made.

For immunohistochemistry, mouse tissue was extracted at P20. Briefly, mice were deeply anesthetized and then killed by perfusion with a solution of 4% paraformaldehyde (wt/vol) and 30% sucrose (wt/vol) in 0.1 mM phosphate buffer. We made 50- μ m sagittal sections of the main olfactory bulb for subsequent processing.

Electrophysiology. Whole-cell recordings were made using patch pipettes filled with an internal buffer (130 mM potassium gluconate, 10 mM HEPES, 2 mM MgCl₂, 2 mM MgATP, 2 mM Na₂ATP, 0.3 mM GTP, 4 mM NaCl and, in some cases, 10–50 μ M Alexa 488/594 Hydrazide or 1% biocytin, wt/vol) using a Multiclamp 700A amplifier (Molecular Devices) and an ITC-18 data acquisition board (Instrutech). Mitral cells were identified under infrared differential interference contrast optics on the basis of their laminar position in the olfactory bulb and their morphology. Cell identity was confirmed with fluorescent intracellular fills that revealed clear apical dendrites that ramified into a single glomerulus. Current-clamp recordings were performed using whole-cell patch pipettes. All experiments were done at 35 °C in Ringer's solution (125 mM NaCl, 25 mM glucose, 2.5 mM KCl, 25 mM NaHCO₃, 1.25 mM NaH₂PO₄, 1 mM MgCl₂ and 2.5 mM CaCl₂) with excitatory (25 μ M AP5 and 10 μ M CNQX) and inhibitory (10 μ M bicuculline) synaptic activity blocked. Additional experiments performed without synaptic blockers were done with Ringer's solution as described above except with a MgCl₂ concentration of 0.2 mM. For all recordings, a 25-pA or 50-pA hyperpolarizing pulse was injected before stimuli were delivered to measure input resistance and membrane time constant, allowing us to track the stability of recordings over multiple trials. When multiple stimuli were presented to mitral cells, trials were interleaved to prevent systematic differences in neural responses that may have arisen over the entire recording epoch.

Immunohistochemistry. We used a monoclonal antibody to a subunit of the voltage-gated K⁺ channel Kv1.2 to characterize differences in channel expression. The monoclonal antibody to Kv1.2 was developed by and obtained from the University of California Davis/US National Institutes of Health NeuroMab Facility. The primary antibody was used at a dilution of 1:1,000 for 1 h. We used an Alexa-Fluor 488-conjugated (Invitrogen) donkey secondary antibody to mouse at a 1:600 dilution for 1 h. For all sections, an additional Hoechst stain to identify cell nuclei was used. Sections were then imaged using a confocal microscope by scanning multiple regions of interest in both the bulb and the mitral cell layer.

Stimulus. Noise traces were generated as previously described²³. Briefly, a 2.5-s white noise current was convolved with an alpha function having a 3-ms rise time (Supplementary Fig. 1). The alpha function was selected as it reflected the time scale for optimal reliability of mitral cell spiking to a fluctuating input²³. Identical input was delivered to all of the cells, causing differences in spiking responses;

including different rates of firing in each cell and different times at which individual spikes occurred even when firing rates were similar (Supplementary Fig. 1). Representative examples of responses to different noise stimuli for another group of cells (Supplementary Fig. 1) illustrated that the response diversity identified (firing rates, spike times, ISI of spikes, etc) were present over various types of stimuli, suggesting that the variability in neuronal responses reflected underlying intrinsic differences across a host of stimuli rather than differences highlighted by selecting a single stimulus.

The variance of the noise used was between 5% and 40% of the direct current (100–800 pA, σ = 20–80 pA) offset for each cell, with the majority of cells receiving 10–20% offset (Supplementary Fig. 1). The variance of the noise was selected as previously described^{23,24} to allow for appropriate estimation of the STA. Specifically, the noise values chosen induced reliable firing in neurons without large input fluctuations. The input fluctuation values chosen were sufficiently small that there was poor correlation between the σ of the input noise and the degree of reliability (R = 0.17) across a fourfold range (5% to 20%) of current (Supplementary Fig. 1). Only when the variance was substantially large did stimulus σ result in effects on cell reliability.

K nearest neighbor analysis. The K nearest neighbor approach was used to classify the 589 spike trains from 15 conditions in eight cells. The same input stimulus was given to all cells with different direct current offsets to induce firing over multiple trials (n = 30–40). For computational efficiency, analysis was performed in the space of the first 15 principal components and because classification accuracy did not change for principal components greater than ten. The original data was then broken up into testing and training sets. The testing sets established the location of known responses in the principal component space and the training sets were probed with respect to these known responses. The Euclidian distance of the unknown response to all known responses was then calculated and the n nearest neighbors were used to determine which cell and condition the unknown spike response belonged to. This process of generating testing and training sets was repeated 20 times, with each repeat reflecting a different random population of testing and training to ensure that the classification accuracy was not a result of artifacts of selecting a single testing/training population.

Information calculation. To generate population responses for our entropy calculations to an identical stimulus, we selected a random group of mitral cells from all of the neurons that received the identical input stimulus. Each of these different populations was considered to be a single diverse mitral cell population. When homogeneous populations were made, spikes drawn at random from a single recorded neurons was assigned for all the cells in the population. When homogeneous populations were generated, random sampling was done with replacement.

Spike trains were then binned into non-overlapping bins of various sizes. If one or more spikes occurred in a bin, then a value of 1 was recorded in that bin. If no spikes occurred in the bin, then a value of 0 was placed in this bin. In bin sizes as large as 12 ms, no examples of bins containing two or more spikes could be found, ensuring that at these bin sizes, the binary strings of 1s and 0s captured the entire spike train. In 16-ms bins, 2.8% of the bins had more than one spike; therefore only time bins of up to 12 ms were considered to ensure that no relevant information was lost in our entropy calculations as a result of doublet spikes.

48. Kapoor, V. & Urban, N.N. Glomerulus-specific, long-latency activity in the olfactory bulb granule cell network. *J. Neurosci.* **26**, 11709–11719 (2006).

49. Urban, N.N. & Sakmann, B. Reciprocal intraglomerular excitation and intra- and interglomerular lateral inhibition between mouse olfactory bulb mitral cells. *J. Physiol. (Lond.)* **542**, 355–367 (2002).